Analytical representation for the ozone electronic ground state potential function in the spectroscopically accessible range and extended vibration predictions

Vladimir G. Tyuterev, Roman V. Kochanov, Sergei A. Tashkun

Proceedings of the International HighRus Conference, St.Petersburg, July 2012
http://symp.iao.ru/en/hrms/17/auxinfo

Analytical representation for the ozone electronic ground state potential function in the spectroscopically accessible range and extended vibration predictions

Vladimir G. Tyuterev

Groupe de Spectrométrie Moléculaire et Atmosphérique
UMR CNRS 7331, UFR Sciences BP 1039, 51687 Reims Cedex 2, France
E-mail: vladimir.tyuterev@univ-reims.fr,

Roman V. Kochanov, Sergei A. Tashkun

Laboratory of Theoretical Spectroscopy, V.E. Zuev Institute of Atmospheric Optics SB RAS
1, Akademician Zuev square, 634021 Tomsk, Russia
E-mail: roman2400@rambler.ru , tashkun@rambler.ru

Abstract

In this work, we give improved vibration band centres predictions for ozone isotopic species including the heterogeneous isotopologues $^{16}O_3$, $^{18}O_3$, and the mixed 16/18 substitutions $^{16}O^{16}O^{18}O$, $^{16}O^{18}O^{16}O$, $^{16}O^{18}O^{18}O$, $^{18}O^{16}O^{18}O$ in the range approaching the dissociation limit. These calculations are performed from the new ozone electronic ground state ozone potential energy surface (PES) of the ozone molecule which is built in two steps. First, *ab initio* electronic energies were computed following the icMRCI-AVXZ ansatz as described by Holka, Szalay, Muller and Tyuterev, *J. Phys. Chem. A* **2010,** *114,* 9927–9935, but with for much dense 3D grid and for extended range of nuclear configurations. These points were fitted with our new analytical model. At the second step lower order PES parameters were empirically optimized in the vicinity of the equilibrium configuration using experimental vibration band centres of $\Delta V \leq 5$ bands of $^{16}O_3$. The predictions with this PES show better accuracy for band centres at higher energies. The improvement appears to be particularly important for the heterogeneous isotopic species. The major aim of this work is providing preliminary information for analyses of ozone isotopic vibration-rotation spectra at high wavenumber range which are currently in progress.

1. Introduction

The accurate determination of the ozone potential energy surfaces (PES) is a prerequisite for spectra analyses at high energy range as well as for theoretical calculations of complex kinetics of formation, dissociation, and recombination of the ozone molecule [1]. Considerable effort has been devoted to the determination of the X^1A_1 ground electronic state PES by ab initio calculations [2-13] or by a fit to experimental rovibrational data[14-16].

Global 3D ab initio ozone surfaces adapted to dynamical calculations have been constructed by Yamashita et al.[6] and by Siebert, Schinke, and Bittererova (SSB PES), [7,8] the latter being actually the most accurate ab initio one built with the internally contracted (ic) multireference configuration interaction method with Davidson correction (icMR-CISD+QD) using cc-pVQZ basis. Babikov et al. [11] and Grebenshchikov et al.[12] used these calculations to study the metastable states and the van der Waals states, respectively. Related dynamical studies have been summarized by Schinke et al in Ref. [1]. Excited electronic ozone states have been considered in [17-22].

The state of art in ab initio studies of the electronic ground state of ozone has been recently reviewed by Holka, Szalay, Muller and Tyuterev [23], who have also given a detailed investigation of various basis and relativistic corrections as well as the extrapolation to the complete basis set limit using in 1D and 2D PES cuts for icMR-CISD and icMR-AQCC methods near the transition state towards the dissociation. An effect of a simultaneous including of 13 singlet electronic states in the CASSCF calculations for a relevant 1D PES cut has been considered by Dawes et al [24] with an implication for ozone kinetics.

Recent analyses of high resolution spectra [25-32] mostly relied on empirical potentials. Up to date, the most accurate empirical PES for the spectroscopic calculations near the open ozone configuration have been determined by Tyuterev, Tashkun et al et al. [14,15] from the fit of FTS experimental vibration–rotation data of $^{16}O_3$ below 5800 cm^{-1}. This PES has been used, for a theoretical interpretation of rates of formation of ozone isotopologues [33], for the assignment of CW-CRDS spectra of $^{16}O_3$ and $^{18}O_3$ [25-32] and for the extrapolation towards highly excited vibrational states [34].

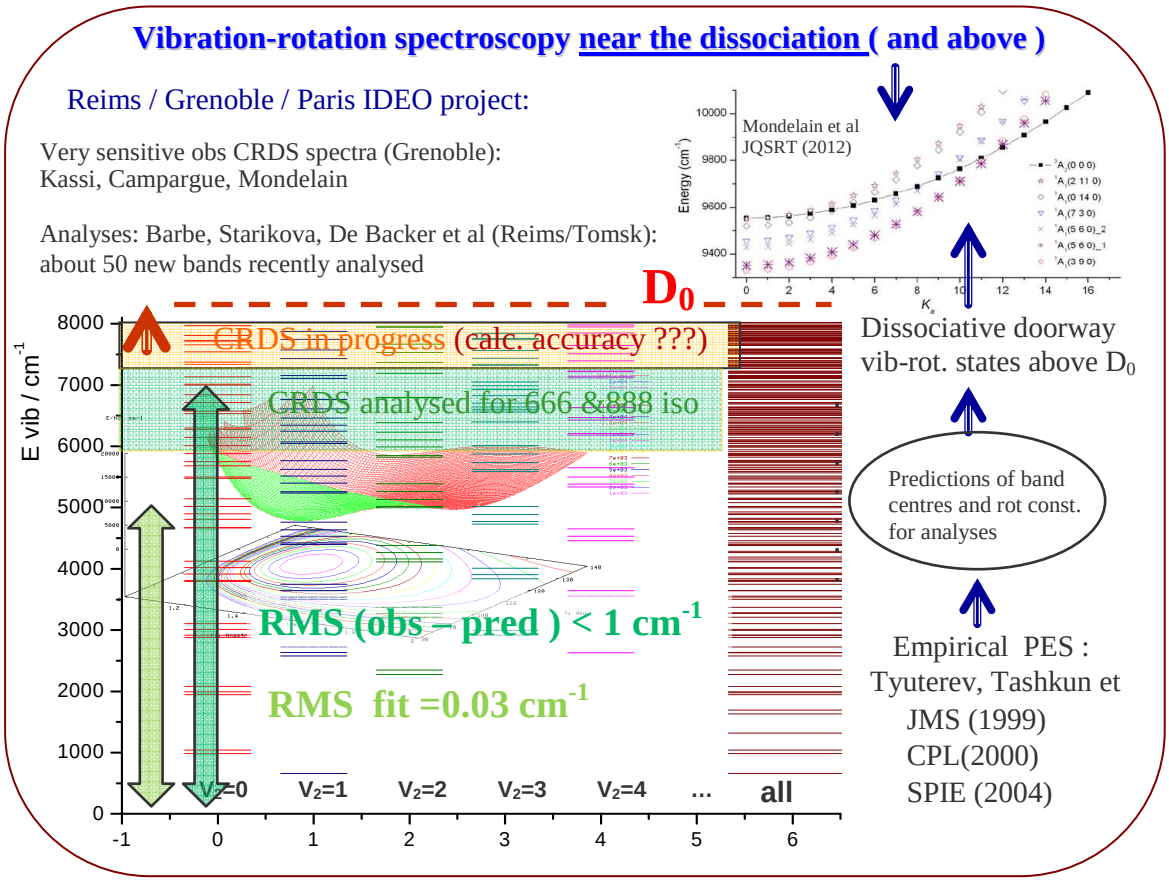

Figure 1. Schematic presentation of the state of art in spectroscopic studies [25-32,34] using our previously determined empirical ozone PES [14-16].

Theoretical calculations for spectroscopic applications and the vibrational assignment of the upper states have been done by two complementary independent methods. One uses variational calculations in internal bond length-bond angle coordinates following Ref. [14-16], the second one employed the method of high order Contact Transformations (CT) in normal coordinates [35, 36] providing full normal mode assignments for all bands. The band center predictions using this PES have been found accurate within 1 cm^{-1} both for $^{16}O_3$ and $^{18}O_3$ [25-30] up to 7000 cm^{-1}, but appeared less reliable at higher energy range and in the case of heterogeneous isotopic substitutions as explained in [14].

Another empirical PES has been obtained [16] through a simultaneous least squares fit to experimental vibration-rotation energy levels of six ozone isotopic species. This PES was the most precise one for rotational calculations as well as for vibrations at low energies resulting in a root mean-square (rms) deviation of 0.02 cm-1 for E/hc < 3800 cm-1**,** and 0.12 cm-1 for E/hc < 4500 cm-1 above the zero-order energy (ZPE) for isotopic data available at that time. Note as an example a recent work [37] where the CT calculation from this PES [16] have allowed building a full Effective Hamiltonian model for the (220)/(121)/(022) triad in the 3000 cm-1 range with very accurate prediction of the entire set of rotational, centrifugal distortion and resonance interaction parameters.

The state of art of spectroscopic applications of global predictions from the electronic ground state ozone PES is schematically represented in Fig 1. As shown in the series of ozone spectra analyses by Barbe et al [25-32], accurate predictions of band centers and rotational constants, in particular for dark perturbing states, are of crucial importance for identifying resonance interactions and for an appropriate set up of the effective Hamiltonian model. A further improvement of the shape of the energy surface is clearly necessary at higher energy range near the dissociation.

2. Extended *ab initio* calculations

The key advantage of the SSB global PES [7,8] is that this surface covers the entire range of nuclear configurations by using the spline interpolation. This also provided correct values of vibration energies, at least for low and medium vibration excitations. For this reason the SSB PES or somewhat modified versions of this PES have been used for the most of studies of ozone dynamics. However these calculations underestimated the GS dissociation limit by about 900 cm^{-1} because of insufficiently large basis set AVQZ with the icMRCI method: larger 3D calculations on the entire grid required for a smooth spline interpolation were at the time of SSB publication too expensive.

In this work we extended icMR-CISD electronic structure calculations with larger complete active space as descried by Holka, Szalay, Muller and Tyuterev [23]. More specifically we computed 3D surfaces with aug-cc-pVXZ(fc) basis sets (abbreviated as AVXZ) , were (fc) invokes the frozen-core approximation with X=Q,5, and 6. Extrapolation Q-5 and 5-6 to the complete basis set (CBS) limit were performed. In addition we have also completed all electron calculations with the ACVQZ basis set for the 3D surface at the main C_{2V} well. Relativistic corrections and size-consistency Davidson and Pople corrections approximately accounting for higher excitations were also explored. This part of the study will be presented in more detail elsewhere [38].

A comparison of the density of the grid points for nuclear configurations of this study around the main C_{2V} equilibrium and along the transition state to the dissociation is shown in Figure 2.

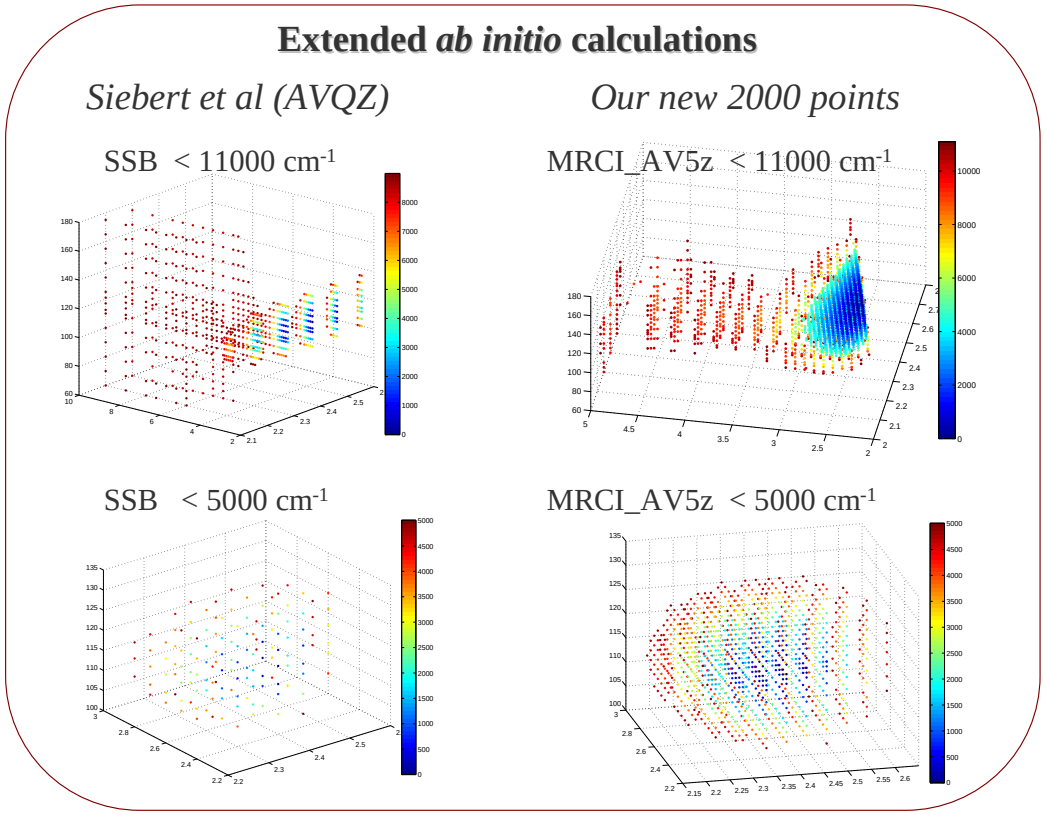

Figure 2. Comparison of the density of nuclear configuration for ab initio electronic ground state energies of the ozone molecule in the previous global PES by Siebert, Schinke, Bittererova (SSB) [7,8] with our recent calculations which are essentially focused on the main potential well and on the way towards the dissociation transition state. The ab initio ansatz corresponds to that of Table I of Holka et al [23].

3. Analytical representation of the PES

A 3D spline PES interpolation has well-known advantages and limitations. An obvious advantage is a possibility of representing complicated shapes of global surfaces. However a reliable 3D spine interpolation requires filling the entire nuclear configuration space by a grid of *ab initio* points even in the ranges which are of no use for spectroscopy or for dynamics. Also this method is very sensitive to outliers due to possible poorly converged points. A physically justified analytical PES representation should be in a sense more robust. This also allows a more flexible choice of the grid by increasing the density of points in the ranges important for spectroscopy applications as shown in Figure 2.

However an investigation of ab initio energies suggested that a standard (morse) × (cosine) analytical parameterization (which was used for most of previous empirical PESs) was not flexible enough for describing a complicated shape of the PES at large internuclear distances. Numerical tests have shown that no other analytical PES representations available

in the literature would be suitable to describe complicated features of the ozone transition states.

In this work we limit our analytical PES representation by the range which is essential for spectroscopy applications: in the vicinity of the main open equilibrium configuration and along the minimum energy path towards the dissociation. As was argued in [14], in order to relate the global potential surface with such an effective potential function , it is convenient to divide the entire vibrational coordinate space r_1, r_2, r_3 into three sectors:

($s1$): $r_2 < r_1$; $r_3 < r_1$ ($s2$): $r_1 < r_2$; $r_3 < r_2$ ($s3$): $r_1 < r_3$; $r_2 < r_3$

The sectors ($s1$), ($s2$), and ($s3$) each have an open structure minimum and all three minima are equivalent. It is clear that it is sufficient to know the potential function within only one of the sectors. An extension to the other sectors can be made by symmetry operations permuting the central nucleus to an "end" position. In the present work, we assume that the potential energy barriers between different C_{2v} minima, and between each C_{2v} minimum and the possible metastable ring structure minimum with $r_1 = r_2 = r_3$, are sufficiently high to be insuperable on the time scale of the experiments with which we are concerned. This assumption is supported by the fact that all available experimental data can be interpreted in terms of asymmetric top effective Hamiltonians which is consistent with one C_{2v} structure for the molecule.

Our analytical representation can be schematically written as follows:

$$V(r_1,r_2,\theta)=\sum_{\substack{i\le j,\\ i+j\le 4}} K_{ij}\,(y_1^{\,i}y_2^{\,j}+y_1^{\,j}y_2^{\,i})+P_n(r_1,r_2,\theta)\,G(r_1,r_2,\theta)$$

Contrary to a usual expansion form (as that of Partridge and Schwenke [39] which was well adapted for H_2O) , our modified curvilinear Morse-type functions

$$y_1=1-\exp(-a\,(r_1-\mu(r_2)))$$

$$y_2=1-\exp(-a\,(r_2-\mu(r_1)))$$

follow the minimum energy path (Figure 3) and account for the shrinking of the bond length (d_{mep}) of the O_2 diatomic fragment on the way to the dissociation:

$$\mu(r)=(\mathrm{r}_0-\mathrm{d}_{mep})\,(1\text{-}\tanh(\mathrm{g}\,(\mathrm{r}\text{-}\mathrm{r}_0)))+\mathrm{d}_{mep}$$

Here r_0 is the O_3 equilibrium band length. $P_n(r_1,r_2,\theta)$ is a correction polynomial

$$P_n(r_1,r_2,\theta)=\sum_{\substack{i,j,k,\\ i+j+k\le n,\\ i\ge j}} C_{ijk}\left(\left(\frac{r_1-r_0}{r_0}\right)^i\left(\frac{r_2-r_0}{r_0}\right)^j+\left(\frac{r_1-r_0}{r_0}\right)^j\left(\frac{r_2-r_0}{r_0}\right)^i\right)\left(\cos(\theta)-\cos(\theta_0)\right)^k$$

and $G(r_1,r_2,\theta)$ is a damping factor:

$$G(r_1,r_2,\theta)=\exp(-g_1\left((r_1-r_0)^2+(r_2-r_0)^2\right)-g_2(r_1-r_0)^2(r_2-r_0)^2-g_3\left(\theta-\theta_0\right)^2)$$

For our ab initio PES at icMRCI-AV5Z level of calculations with Pople and relativistic corrections we have obtained r_0 = 2.409547 *borh* and θ_0 = 116.7772 °.

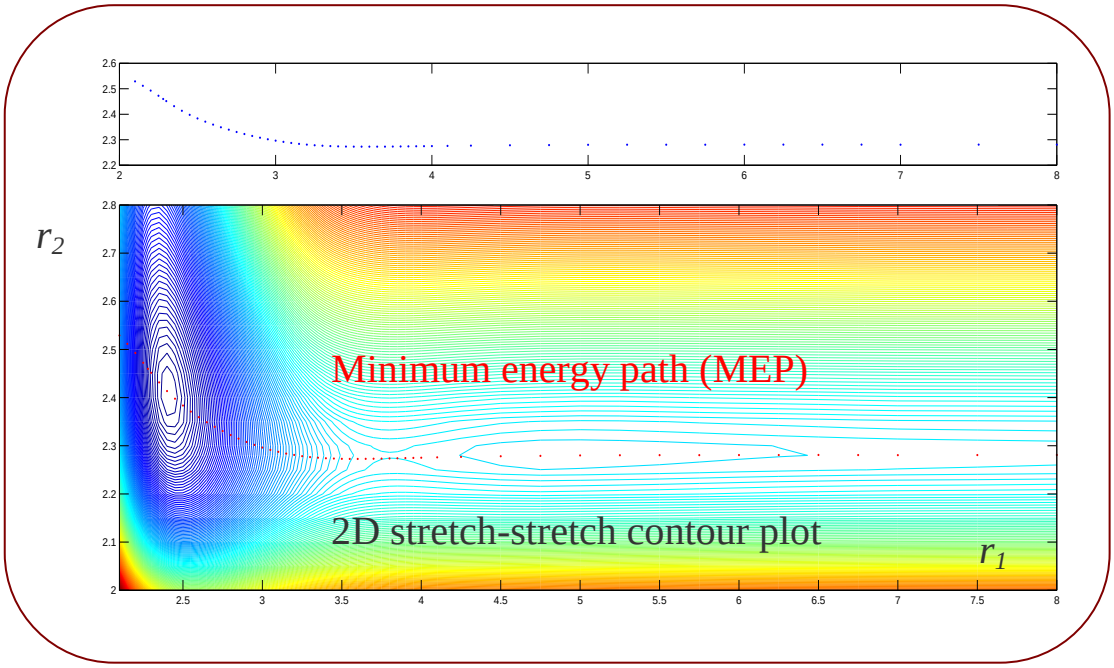

Figure 3. The 2D representation of the minimum energy path (MEP) to the ozone dissociation in the electronic ground state with our PES. The apex angle if fixed to 117 ° (near equilibrium value). The bond lengths R1 and R2 are given in bohr.

Note ones again that this form represents a shape of the PES in one of the sectors (s_i) and neglects the ring structure well which is much higher in energy and is not thus accessible in usual experimental conditions.

4. Variational and DVR calculations

There exist various implementations of global methods of calculations in molecular spectroscopy. A common feature is a numerical solution of the quantum mechanical eigenvalue problem for the Hamiltonian depending on $3N - 3$ suitably chosen rovibrational coordinates. A variational approach (see [39-44,14-16] and references therein) with basis optimization and matix truncation-compression technique is usually applied. A discrete variable representation (DVR) [45-48] and filter-digitalization [49] techniques aimed at improvement of a basis convergence for high-energy range are also widely used. Global methods offer complementary possibilities as compared to traditional band-by-band or polyad-by-polyad effective Hamiltonian models. A comparison of specific advantages and problems of these two approaches in molecular spectroscopy have been recently discussed in [50].

In order to compute vibration–rotation energies from the exact kinetic energy (EKE) Hamiltonian, we use the methods and computer codes in the same way as described in our previous papers on global calculations for the ozone molecule (see [14-16] for more details). In order to confirm the results by two independent EKE-methods, we have performed

calculations both with the DVR and variational methods which we were able to converge to nearly to the same values at least up to 7500 cm^{-1}.

5. Empirical optimisation at low energies

Pure ab initio PESs computed with various ansatze outlined above in section 2 give quite closed results for lower vibrational levels in a reasonable agreement with experimental data. An example of the effect of basis corrections and of CBS limit on the main expansion coefficients in a polynomial approximation is given in Table 1. The results of the pure ab initio calculations will be reported elsewhere [38].

Parameter	AVQZ	AV5Z	AV6Z	AVX5_CBS	ACVQZ
C 002	0.3321E+05	0.3332E+05	0.3340E+05	0.3344E+05	0.3360E+05
C 101	-0.3271E+05	-0.3291E+05	-0.3307E+05	-0.3313E+05	-0.3331E+05
C 110	0.6237E+05	0.6236E+05	0.6234E+05	0.6236E+05	0.6189E+05
C 200	0.2460E+06	0.2480E+06	0.2489E+06	0.2501E+06	0.2491E+06

Table 1: Effect of basis corrections and of CBS limit on the main expansion coefficients in a polynomial approximation in the vicinity of the main well if only $P_n(r_1,r_2,\theta)$ is used for the PES fit withour damping factor and without the Morse terms. All versions account for Pople and relativistic corrections.

Here we just mention that in general, for all icMRCI-AVXZ calculations the bending levels are somewhat underestimated (as already discussed in [23]) whereas stretching levels tend to overestimate experimental values when the cardinal number X increases. The main purpose of this work was to build an optimized PES for spectroscopic applications at high energy range. To this end we adjusted lower order polynomial parameters in the correction terms (second term in our PES representation) which are responsible for the PES fine tuning near the equilibrium configuration. Only 19 parameters for $n < 4$ terms were fitted to experimental vibration band centres of $\Delta V \leq 5$ bands of $^{16}O_3$ which were very well defined from FTS ozone spectra [51]. This represents only 11% of the total number (168) of PES parameters. All "frame" terms (first term in our PES representation) which are responsible for the surface behaviour at large internuclear distances were kept fixed to the values determined from *ab initio* points at the first step of calculations.

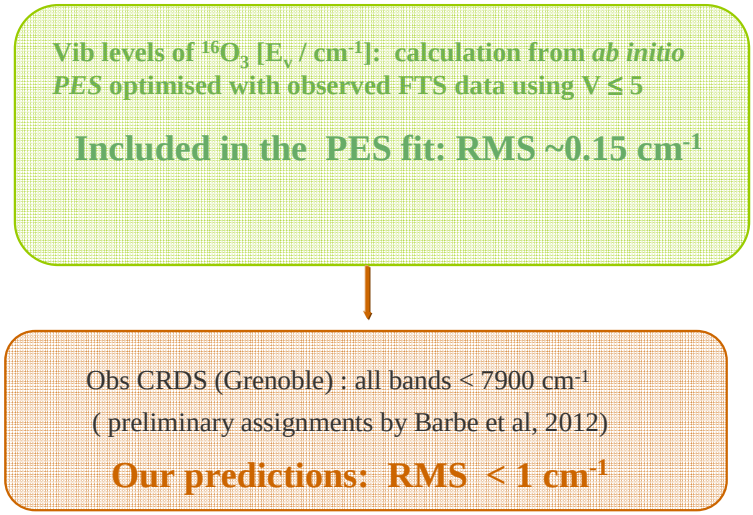

Figure 4. A scheme of empirical optimisation adopted for our PES

For the empirical optimisation we used the same technique of flexible constraints as described in [14-15]. The results of the fit are schematically represented in Figure 4. The stretch-stretch cuts of our empirically optimized PES for various bond-bond angles is given in Figures 5a-5c. The dissociation limit of this PES (D_0 = 1.096 eV) is somewhat overestimated. At the current state this PES shows physically meaningful shape up to 10000-12000 cm^{-1} which is the most important range for spectra analyses. This means the range of internuclear distances covered by wave functions of quantum states which could be actually accessible by spectroscopic high-resolution experiments: in segments {1.9 bohr < r_1 < 3 bohr with 1.9 bohr < r_2 < 20 bohr } or symmetrically {1.9 bohr < r_2 < 3 bohr with 1.9 bohr < r_1 < 20 bohr }. The apex angle variations is expected to be reliably described in the range 90° < θ < 135° in the main potential well.

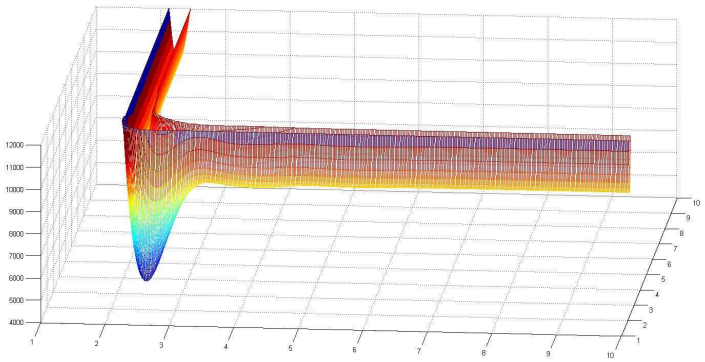

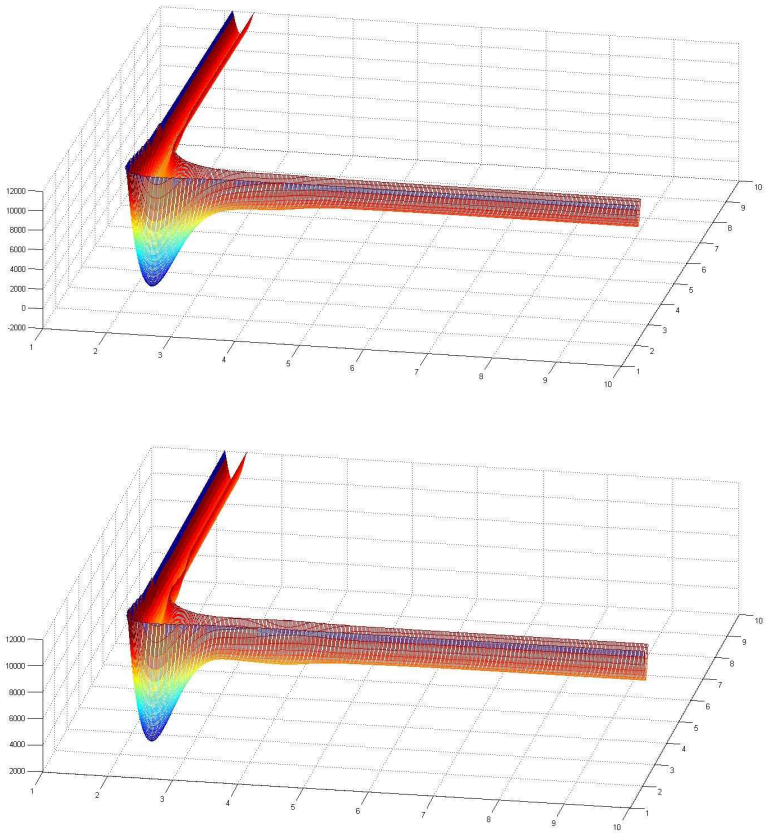

Figures 5a-5c: The stretch-stretch cuts of our empirically optimized PES for the bond-bond angles 100°, 117° and 130°. Horizontal axes: r_1 and r_2 /bohr; vertical axis: PES /cm^{-1}

This PES does not yet have a perfect shape in the entire range of nuclear configurations: in particular it shows some artefacts on the r_1/r_2 bisector cut (though for energies more than twice higher than the dissociation threshold) and for very low apex angles. We hope to be able improving this behaviour for dynamical applications at the next update and thus consider the results as preliminary ones. However these features should not have a considerable impact on vibrational predictions which are useful for current analyses of vibration-rotation spectra.

6. Vibration band centres predictions.

It is well known [52] that for A-type vibration states of C_{2V} ozone species containing ^{16}O and ^{18}O isotopes the J=0 rovibration levels are not allowed by nuclear spin statistics. However in experimental spectra analyses a band centre is traditionally defined as $J \rightarrow 0$ limit of rovibrational upper state levels. This limit could be experimentally determined from spectra by following transition series in P, Q or R branches in a sufficiently large range of J, Ka values. For this reason it is instructive to calculate theoretical values for the band centres. The values for the centres of bands (N'=0, A) $\rightarrow$ (N,Γ) computed with exact kinetic energy operator and the DVR method using our new empirically optimized PES are given in the Appendices A-D. Here N' and N are global vibration ranking numbers for the low and upper states, Γ is a vibration symmetry type of the upper vibrations state and (N'=0, A) stands for the ground vibration state: A=A_1 for C_{2V} species and A=A' for C_s species. Atomic masses are used in the calculations.

Note that these are yet preliminary results that aim at helping current experimental spectra analyses in high energy range for various ozone isotopic species.

Further improvement of our PES at large internuclear distances is in progress.

7. Acknowledgements

We acknowledge the support from ANR "IDEO" and LEFE-CHAT CNRS grants, from Balaton French-Hungarian PHC exchange program, from IDRIS/CINES computer centers of France and of the computer center "Clovis" Reims-Champagne-Ardenne Region of France. We are indebted to P.Szalay, F.Holka, T.Muller and R.Schinke for collaboration and discussions on quantum chemistry calculations as well as to D.Schwenke and M.Jacon for collaboration in variational methods. Our special thanks are for A.Barbe, E.Starikova, S.Mikhailenko, M.R. De Backer, X.Thomas, S.Kassi, D.Mondelain, R.Jost and A.Campargue for stimulating works on ozone spectra measurements and analyses.

References

[1] Schinke, R.; Grebenshchikov, S. Y.; Ivanov, M. V.; Fleurat-Lessard, P. Annu. ReV. Phys. Chem. 2006, 57, 625.
[2] Banichevich, A.; Peyerimhoff, S. D.; Grein, F. Chem. Phys. 1993, 178, 155.
[3] Borowski, P.; Flscher, M.; Malmquist, P. A.; Roos, B. O. Chem. Phys. Lett. 1995, 237, 195.
[4] Xantheas, S.; Atchity, G.; Elbert, S.; Ruedenberg, K. J. Chem. Phys. 1991, 94, 8054.
[5] Xie, D.; Guo, H.; Peterson, K. A. J. Chem. Phys. 2000, 112, 8378.
[6] Yamashita, K.; Morokuma, K.; Quere, F. L.; Leforestier, C. Chem.Phys. Lett. 1992, 191, 515–520.
[7] Siebert, R.; Schinke, R.; Bittererova, M. Phys. Chem. Chem. Phys.2001, 3, 1795.
[8] Siebert, R.; Fleurat-Lessard, P.; Schinke, R.; Bittererova, M.; Farantos, S. C. J. Chem. Phys. 2002, 116, 9749.
[9] Schinke, R.; Fleurat-Lessard, P. J. Chem. Phys. 2004, 121, 5789.
[10] Fleurat-Lessard, P.; Grebenshchikov, S.; Siebert, R.; Schinke, R.;Halberstadt, N. J. Chem. Phys. 2003, 118, 610.
[11] Babikov, D.; Kendrick, B.; Walker, R. B.; Pack, R.; Fleurat-Lesard, P.; Schinke, R. J. Chem. Phys. 2003, 118, 6298.
[12] Grebenshchikov, S. Y.; Schinke, R.; Fleurat-Lessard, P.; Joyeux, M. J. Chem. Phys. 2003, 119, 6512.
[13] Tashiro, M.; Schinke, R. J. Chem. Phys. 2003, 119, 10186.
[14] Tyuterev, Vl. G.; Tashkun, S.; Jensen, P.; Barbe, A. J. Mol. Spectrosc. 1999, 198, 57.
[15] Tyuterev, Vl. G.; Tashkun, S.; Schwenke, D. W.; Jensen, P.; Cours, T.; Barbe, A.; Jacon, M. Chem. Phys. Lett. 2000, 316, 271.
[16] Tyuterev, Vl. G.; Tashkun, S. A.; Schwenke, D.; Barbe, A. SPIE Proc. Ser., 2004, 5311, 176–184.
[17] Rosmus, P.; Palmieri, P.; Schinke, R. J. Chem. Phys. 2002, 117, 4871.
[18] Grebenshchikov, S. Y.; Schinke, R. J. Chem. Phys. 2009, 131, 181103.
[19] Qu, Z. W.; Zhu, H.; Grebenshchikov, S.; Schinke, R.; Farantos, S. J. Chem. Phys. 2006, 124, 204313.
[20] Grebenshchikov, S. Y.; Schinke, R.; Qu, Z. W.; H, Zhu J. Chem.Phys. 2006, 124, 204313.
[21] Grebenshchikov, S. Y.; Qu, Z. W.; Schinke, R. Phys. Chem. Chem.Phys. 2007, 9, 2044.
[22] Ndengue, S; Gatti, F; Meyer,H.D; Schinke, R; and Jost,R, Workshop "Spectroscopy and

dynamics of ozone and related atmospheric species" , REIMS, FRANCE, 3-5 October 2011

[23] Holka,F; Szalay,P; Muller,T; Tyuterev, Vl.G, J. Phys. Chem. A, 2010, 114, 9927-9935

[24 Dawes,R; Lolur, P; Ma.J; Guo, H, J. Phys. Chem. A, 2011, 135, 081102-081106

[25] Barbe, A.; De Backer-Barilly, M.-R. D.; Tyuterev, Vl. G.; Kassi, S.; Campargue, A. J. Mol. Spectrosc. 2007, 246, 22–38.
[26] Campargue, A.; Barbe, A.; De Backer-Barilly, M.-R. ; Tyuterev, Vl.G.; Kassi, S. Phys. Chem. Chem. Phys. 2008, 10, 2925–2946.
[27] Campargue, A.; Liu, A. W.; Kassi, S.; De Backer-Barilly, M.-R.; Barbe, A.; Starikova, E.; Tashkun, S. A.; Tyuterev, Vl. G. J. Mol. Spectrosc.2009, 255, 75–87.
[28] Starikova, E.; De Backer-Barilly, M.-R. ; Barbe, A.; Tyuterev, Vl.G.; Campargue, A.; Liu, A. W.; Kassi, S. J. Mol. Spectrosc. 2009, 255, 144–156.
[29] Starikova, E.; Barbe, A.; Tyuterev, Vl. G.; De Backer-Barilly, M.-R.; Kassi S.; Campargue, A. J. Mol. Spectrosc. 2009, 257, 40–56.
[30] Starikova E, Barbe A, De Backer-Barilly M.R, Tyuterev Vl.G, Tashkun S.A, Kassi S, Campargue A. Chem Phys Lett 2009;470:28-34
[31] Mondelin, D; Campargue, A; Kassi, S; Barbe, A; Starikova, E; De Backer-Barilly, M.R; Tyuterev, Vl.G; J Quant Spectrosc Radiat Transfer, to be published
[32] Starikova, E; Barbe, A; De Backer, M.R; Tyuterev, Vl.G; Mondelain, D; Kassi. S; Campargue, A, J Quant Spectrosc Radiat Transfer 2012;113:1741–1752
[33] Miklavc, A, Peyerimhoff, S, Chem. Phys. Lett. 359 [2002] 55.
[34] Mondelain ,D; Jost,R; Kassi,S; Judge, R.H ;Tyuterev Vl.G, , and Campargue, A, JQSRT 2012, 113, 840-849,
[35] Tyuterev, Vl. G.; Tashkun, S. A.; Seghir, SPIE Proc. Ser., 2004; Vol. 5311, p 164-175.
[36] Lamouroux, J.; Tashkun, S. A.; Tyuterev, Vl. G. Chem Phys Lett 2008, 452, 225-231.
[37] Barbe, A ; De Backer-Barilly, M.-R; Starikova, E; Tashkun S.A; Thomas, X; Tyuterev Vl.G,/ Journal of Quantitative Spectroscopy & Radiative Transfer 2012, 113, 829–839
[38] Tyuterev, Vl.G; Kochanov,R; Tashkun S.A; Holka,F; Szalay,P; in preparation
[39] Partridge,H; Schwenke,D.W, J. Chem. Phys. 1997, 106, 4618–4639.
[40] Carter, S; Handy,N; J. Chem. Phys. 1987,87, 4294–4301.
[41] Jensen,P, J. Mol. Spectrosc. 1988,128, 478–501.
[42] Schwenke, D.W, J. Phys. Chem. 1996, 100, 2867–2884.
[43] Yurchenko,S; Barber,R; Tennyson,J; Thiel,W; and Jensen,P; J. Mol. Spectrosc.2011, 268, 123-129
[44] Alijah, A; Varandas,A; J.Chem.Phys A, 2006, 110(16) 5499-5503
[45] Tennyson,J; Miller,S; Henderson,J, in: S. Wilson [Ed.], Methods in Computational Chemistry, vol. 4, Plenum, New York, 1992.
[46] Choi,S; Light,J, J. Chem. Phys. 1992,97, 7031–7054.
[47] Light,J; Carrington, T, Adv.Chem.Phys, 2000, 114, 263
[48] Zobov,N; Shirin,S; Lodi,L; Tennyson,J; Csaszar,A and Polyansky,O, Chem. Phys. Letts., 2011, 507, 48-51
[49] Mandelstam, V.A.; Taylor, H.S, J. Chem. Phys. 1997, 106, 5085–5090.
[50] Tyuterev, Vl.G, Atmos. Ocean. Opt. ,2003, 16, 220–230
[51] Babikov, Y; Mikhailenko. S; Tyuterev, Vl.G; Barbe, A, Spectroscopy and molecular properties of ozone; http://www.ozone.univ-reims.fr and http://www.ozone.iao.ru
[52] Flaud, J.M; Bacis, R, Spectrochimica Acta A, 1998, 54, 3-16.

Appendix A. Vibrational band centres for the 16O3 ozone isotopologue using EKE Hamiltonian, DVR method and emprically optimised PES Tyuterev, Kochanov,Tashkun (model_mep1, September 2011)
All values in cm-1; Cut-off: 8000 cm-1

species	666		666
zpe	1443.667		
2 A	701.070	1 B	1041.888
3 A	1103.080	2 B	1726.463
4 A	1399.391	3 B	2110.812
5 A	1796.321	4 B	2407.864
6 A	2057.747	5 B	2785.361
7 A	2094.945	6 B	3046.072
8 A	2201.052	7 B	3086.002
9 A	2486.609	8 B	3186.345
10 A	2726.043	9 B	3455.911
11 A	2787.693	10 B	3698.269
12 A	2886.173	11 B	3760.742
13 A	3083.768	12 B	3849.937
14 A	3173.810	13 B	4021.870
15 A	3289.925	14 B	4122.003
16 A	3390.798	15 B	4250.155
17 A	3477.594	16 B	4346.575
18 A	3568.022	17 B	4431.916
19 A	3739.572	18 B	4508.139
20 A	3857.714	19 B	4659.029
21 A	3966.718	20 B	4782.952
22 A	4001.371	21 B	4897.294
23 A	4051.959	22 B	4919.179
24 A	4141.388	23 B	4990.968
25 A	4164.590	24 B	5077.171
26 A	4246.125	25 B	5099.299
27 A	4370.026	26 B	5159.233
28 A	4390.575	27 B	5291.208
29 A	4537.983	28 B	5307.744
30 A	4632.899	29 B	5437.728
31 A	4643.827	30 B	5518.966
32 A	4709.492	31 B	5559.169
33 A	4783.525	32 B	5631.393
34 A	4848.612	33 B	5697.434
35 A	4919.500	34 B	5762.572
36 A	4922.514	35 B	5783.596
37 A	5036.181	36 B	5800.237
38 A	5039.021	37 B	5919.040
39 A	5171.863	38 B	5947.107
40 A	5214.029	39 B	6063.642
41 A	5265.451	40 B	6084.749
42 A	5310.039	41 B	6124.557
43 A	5363.475	42 B	6198.234
44 A	5418.647	43 B	6267.617
45 A	5440.989	44 B	6305.172
46 A	5529.565	45 B	6355.774
47 A	5540.913	46 B	6386.795
48 A	5585.780	47 B	6420.797
49 A	5678.361	48 B	6427.087
50 A	5701.826	49 B	6543.003
51 A	5766.404	50 B	6567.898
52 A	5813.148	51 B	6586.867
53 A	5884.766	52 B	6687.190

species	666		666
54 A	5889.839	53 B	6716.676
55 A	5970.774	54 B	6721.803
56 A	5995.082	55 B	6828.396
57 A	6014.276	56 B	6880.304
58 A	6046.020	57 B	6895.463
59 A	6100.758	58 B	6898.583
60 A	6154.700	59 B	6982.174
61 A	6205.168	60 B	6989.615
62 A	6207.322	61 B	7033.156
63 A	6238.998	62 B	7075.102
64 A	6319.417	63 B	7081.522
65 A	6343.616	64 B	7130.307
66 A	6365.588	65 B	7159.164
67 A	6443.787	66 B	7188.538
68 A	6502.838	67 B	7286.239
69 A	6505.850	68 B	7309.591
70 A	6548.117	69 B	7343.372
71 A	6566.304	70 B	7344.277
72 A	6614.456	71 B	7395.350
73 A	6627.256	72 B	7445.333
74 A	6662.801	73 B	7450.753
75 A	6669.144	74 B	7486.182
76 A	6751.218	75 B	7517.356
77 A	6764.594	76 B	7577.549
78 A	6818.748	77 B	7591.449
79 A	6869.650	78 B	7616.866
80 A	6881.753	79 B	7660.459
81 A	6917.135	80 B	7684.854
82 A	6929.149	81 B	7721.974
83 A	6964.535	82 B	7737.555
84 A	6999.216	83 B	7757.407
85 A	7075.023	84 B	7778.933
86 A	7107.728	85 B	7836.848
87 A	7121.639	86 B	7857.863
88 A	7152.309	87 B	7928.443
89 A	7200.325	88 B	7943.666
90 A	7224.843	89 B	7962.393
91 A	7225.939	90 B	7993.360
92 A	7235.123		
93 A	7288.942		
94 A	7310.338		
95 A	7343.960		
96 A	7366.586		
97 A	7379.935		
98 A	7436.824		
99 A	7472.093		
100 A	7478.613		
101 A	7538.036		
102 A	7552.471		
103 A	7556.315		
104 A	7599.538		
105 A	7607.212		
106 A	7653.246		
107 A	7682.924		
108 A	7716.278		
109 A	7716.885		
110 A	7785.349		
111 A	7804.985		
112 A	7811.641		

species		666	666
113	A	7835.812	
114	A	7844.102	
115	A	7863.983	
116	A	7887.218	
117	A	7946.303	
118	A	7948.346	
119	A	7955.489	
120	A	7966.794	

Appendix B. Vibrational band centres for the 18O3 ozone isotopologue using EKE Hamiltonian, DVR method and emprically optimised PES Tyuterev, Kochanov,Tashkun (model_mep1, September 2011)
All values in cm-1; Cut-off: 8000 cm-1

species	888		888
zpe	1361.101		
2 A	661.655	1 B	984.639
3 A	1041.495	2 B	1631.700
4 A	1320.876	3 B	1996.021
5 A	1696.253	4 B	2275.984
6 A	1946.332	5 B	2634.405
7 A	1977.651	6 B	2883.887
8 A	2078.275	7 B	2917.427
9 A	2348.428	8 B	3012.514
10 A	2578.975	9 B	3269.401
11 A	2631.951	10 B	3502.285
12 A	2725.904	11 B	3555.927
13 A	2920.082	12 B	3641.490
14 A	2997.927	13 B	3813.533
15 A	3107.078	14 B	3900.687
16 A	3208.533	15 B	4019.283
17 A	3283.744	16 B	4117.312
18 A	3370.734	17 B	4191.363
19 A	3542.051	18 B	4266.142
20 A	3644.606	19 B	4419.099
21 A	3747.492	20 B	4527.798
22 A	3792.859	21 B	4637.032
23 A	3834.960	22 B	4666.916
24 A	3919.591	23 B	4728.954
25 A	3932.989	24 B	4808.745
26 A	4012.462	25 B	4823.579
27 A	4128.074	26 B	4885.380
28 A	4159.940	27 B	5019.623
29 A	4288.245	28 B	5020.979
30 A	4383.755	29 B	5150.050
31 A	4397.756	30 B	5239.318
32 A	4458.209	31 B	5266.139
33 A	4529.907	32 B	5337.192
34 A	4579.634	33 B	5400.709
35 A	4650.521	34 B	5452.362
36 A	4674.124	35 B	5497.333
37 A	4761.202	36 B	5499.243
38 A	4773.592	37 B	5617.267
39 A	4897.554	38 B	5629.236
40 A	4928.483	39 B	5748.784
41 A	4994.704	40 B	5766.421
42 A	5020.054	41 B	5822.008
43 A	5078.291	42 B	5871.906
44 A	5134.603	43 B	5941.977
45 A	5140.986	44 B	5984.638
46 A	5223.614	45 B	6013.140
47 A	5263.042	46 B	6072.222
48 A	5283.687	47 B	6077.384
49 A	5382.775	48 B	6099.093
50 A	5390.598	49 B	6210.781
51 A	5480.376	50 B	6228.142
52 A	5511.579	51 B	6270.754
53 A	5564.689	52 B	6342.914

species		888			888
54	A	5590.127	53	B	6375.352
55	A	5648.001	54	B	6392.621
56	A	5682.466	55	B	6472.950
57	A	5695.361	56	B	6531.286
58	A	5733.085	57	B	6542.982
59	A	5766.604	58	B	6557.018
60	A	5847.525	59	B	6611.306
61	A	5864.843	60	B	6642.901
62	A	5876.671	61	B	6686.050
63	A	5908.986	62	B	6698.770
64	A	5989.527	63	B	6712.250
65	A	6012.226	64	B	6796.642
66	A	6047.406	65	B	6800.548
67	A	6108.220	66	B	6825.632
68	A	6145.654	67	B	6929.402
69	A	6179.565	68	B	6950.649
70	A	6195.702	69	B	6974.682
71	A	6245.323	70	B	6997.535
72	A	6266.489	71	B	7009.059
73	A	6296.167	72	B	7065.184
74	A	6309.898	73	B	7101.297
75	A	6326.163	74	B	7115.334
76	A	6386.282	75	B	7138.803
77	A	6427.937	76	B	7194.455
78	A	6462.696	77	B	7210.830
79	A	6503.199	78	B	7255.597
80	A	6519.939	79	B	7277.178
81	A	6573.219	80	B	7314.760
82	A	6593.006	81	B	7325.591
83	A	6597.525	82	B	7369.652
84	A	6633.561	83	B	7378.418
85	A	6704.353	84	B	7393.586
86	A	6760.584	85	B	7486.308
87	A	6762.985	86	B	7502.645
88	A	6788.738	87	B	7527.863
89	A	6819.363	88	B	7560.228
90	A	6845.130	89	B	7576.525
91	A	6862.843	90	B	7627.934
92	A	6869.413	91	B	7647.580
93	A	6919.213	92	B	7655.807
94	A	6922.868	93	B	7666.121
95	A	6989.122	94	B	7716.001
96	A	7004.804	95	B	7720.228
97	A	7011.914	96	B	7751.420
98	A	7048.274	97	B	7766.375
99	A	7109.517	98	B	7803.914
100	A	7132.094	99	B	7833.326
101	A	7138.561	100	B	7854.240
102	A	7142.566	101	B	7906.354
103	A	7156.209	102	B	7924.914
104	A	7208.277	103	B	7932.918
105	A	7225.105	104	B	7948.971
106	A	7302.384	105	B	7975.349
107	A	7311.278	106	B	7987.450
108	A	7327.159	107	B	8013.119
109	A	7337.631			
110	A	7372.267			
111	A	7429.936			
112	A	7430.580			

species	888	888
113 A	7432.571	
114 A	7439.206	
115 A	7497.755	
116 A	7519.261	
117 A	7535.319	
118 A	7538.113	
119 A	7559.050	
120 A	7581.171	
121 A	7639.319	
122 A	7662.478	
123 A	7674.972	
124 A	7707.703	
125 A	7734.866	
126 A	7749.986	
127 A	7770.599	
128 A	7775.249	
129 A	7803.966	
130 A	7808.577	
131 A	7824.657	
132 A	7866.577	
133 A	7882.961	
134 A	7910.502	
135 A	7951.171	
136 A	7957.641	
137 A	7973.756	
138 A	8017.270	

Appendix C. Vibrational band centres for the 16O18O16O
ozone isotopomer
using EKE Hamiltonian, DVR method and emprically optimised PES
Tyuterev, Kochanov,Tashkun (model_mep1, September 2011)
All values in cm-1; Cut-off: 7000 cm-1

species	686		686
zpe	1407.033		
2 A	693.439	1 B	1008.2683
3 A	1074.284	2 B	1686.4254
4 A	1384.216	3 B	2049.4663
5 A	1760.202	4 B	2361.5665
6 A	1992.905	5 B	2718.1419
7 A	2072.313	6 B	2952.4270
8 A	2143.385	7 B	3033.6123
9 A	2443.281	8 B	3095.7233
10 A	2655.919	9 B	3383.0851
11 A	2757.703	10 B	3600.4387
12 A	2821.557	11 B	3702.4591
13 A	2993.038	12 B	3754.1135
14 A	3123.402	13 B	3904.4194
15 A	3204.064	14 B	4043.8997
16 A	3315.632	15 B	4131.8132
17 A	3440.353	16 B	4244.8904
18 A	3496.572	17 B	4367.9728
19 A	3644.408	18 B	4407.4176
20 A	3800.385	19 B	4538.6794
21 A	3873.582	20 B	4700.0028
22 A	3882.420	21 B	4765.2776
23 A	3971.998	22 B	4785.5283
24 A	4020.514	23 B	4885.7804
25 A	4120.217	24 B	4927.7553
26 A	4167.984	25 B	5029.9742
27 A	4256.409	26 B	5054.0262
28 A	4291.443	27 B	5161.5658
29 A	4473.935	28 B	5168.7209
30 A	4513.221	29 B	5350.5194
31 A	4541.931	30 B	5379.1315
32 A	4625.008	31 B	5427.7809
33 A	4659.088	32 B	5523.1200
34 A	4780.937	33 B	5545.6513
35 A	4797.240	34 B	5620.5443
36 A	4834.846	35 B	5688.0264
37 A	4918.572	36 B	5691.3289
38 A	4934.163	37 B	5795.1799
39 A	5025.229	38 B	5796.5930
40 A	5141.250	39 B	5891.6809
41 A	5143.543	40 B	5983.9814
42 A	5203.767	41 B	5994.1413
43 A	5274.757	42 B	6063.4182
44 A	5291.276	43 B	6151.6562
45 A	5300.118	44 B	6156.9513
46 A	5398.253	45 B	6182.5103
47 A	5471.348	46 B	6225.1946
48 A	5494.827	47 B	6314.4780
49 A	5573.071	48 B	6342.5124
50 A	5575.301	49 B	6396.4765
51 A	5606.537	50 B	6418.7700

species	686		686
52 A	5660.702	51 B	6422.8427
53 A	5764.091	52 B	6513.7245
54 A	5808.269	53 B	6577.8255
55 A	5819.747	54 B	6628.8137
56 A	5857.336	55 B	6684.7910
57 A	5916.972	56 B	6689.2345
58 A	5921.757	57 B	6741.2846
59 A	5953.505	58 B	6786.4289
60 A	6012.122	59 B	6803.5601
61 A	6031.351	60 B	6830.5576
62 A	6142.109	61 B	6882.4403
63 A	6142.598	62 B	6920.0772
64 A	6189.798	63 B	6955.7919
65 A	6212.866	64 B	6992.1100
66 A	6226.436	65 B	7026.5182
67 A	6290.745		
68 A	6335.169		
69 A	6380.277		
70 A	6387.959		
71 A	6446.614		
72 A	6466.330		
73 A	6490.982		
74 A	6542.145		
75 A	6566.530		
76 A	6595.323		
77 A	6623.782		
78 A	6645.306		
79 A	6731.164		
80 A	6765.720		
81 A	6769.521		
82 A	6810.404		
83 A	6855.452		
84 A	6856.585		
85 A	6924.073		
86 A	6946.353		
87 A	6977.130		
88 A	6985.479		
89 A	7027.580		

Appendix D. Vibrational band centres for the the 16O18O16O ozone isotopolomer
using EKE Hamiltonian, DVR method and emprically optimised PES
Tyuterev, Kochanov,Tashkun (model_mep1, September 2011)
All values in cm-1; Cut-off: 7000 cm-1

species	868		868
zpe	1398.582		
2 A	668.251	1 B	1019.159
3 A	1072.123	2 B	1671.680
4 A	1333.994	3 B	2060.052
5 A	1733.201	4 B	2321.287
6 A	1997.185	5 B	2703.412
7 A	2013.029	6 B	2967.823
8 A	2139.548	7 B	2980.466
9 A	2391.604	8 B	3107.398
10 A	2649.902	9 B	3343.170
11 A	2658.017	10 B	3601.846
12 A	2793.142	11 B	3611.733
13 A	3014.399	12 B	3740.711
14 A	3047.233	13 B	3935.561
15 A	3198.279	14 B	3978.974
16 A	3283.726	15 B	4143.506
17 A	3316.001	16 B	4220.086
18 A	3443.851	17 B	4251.863
19 A	3640.022	18 B	4369.468
20 A	3699.916	19 B	4543.349
21 A	3844.387	20 B	4610.282
22 A	3913.624	21 B	4765.783
23 A	3916.973	22 B	4814.194
24 A	3971.407	23 B	4834.586
25 A	4045.267	24 B	4888.669
26 A	4091.354	25 B	4963.425
27 A	4248.716	26 B	4992.535
28 A	4261.199	27 B	5146.138
29 A	4349.409	28 B	5173.887
30 A	4486.900	29 B	5236.311
31 A	4522.700	30 B	5376.499
32 A	4541.342	31 B	5409.146
33 A	4624.110	32 B	5445.308
34 A	4658.417	33 B	5521.790
35 A	4735.049	34 B	5556.964
36 A	4821.325	35 B	5607.903
37 A	4877.424	36 B	5669.024
38 A	4887.438	37 B	5744.111
39 A	4995.308	38 B	5786.148
40 A	5050.683	39 B	5855.888
41 A	5118.281	40 B	5928.039
42 A	5131.815	41 B	5964.971
43 A	5164.903	42 B	6012.078
44 A	5265.546	43 B	6052.158
45 A	5274.024	44 B	6141.926
46 A	5290.519	45 B	6150.842
47 A	5373.683	46 B	6195.287
48 A	5410.805	47 B	6212.329
49 A	5489.124	48 B	6240.430
50 A	5521.902	49 B	6337.669
51 A	5636.903	50 B	6388.723
52 A	5641.175	51 B	6457.352

species		868			868
53	A	5676.000	52	B	6467.221
54	A	5717.779	53	B	6524.383
55	A	5762.249	54	B	6536.069
56	A	5785.324	55	B	6614.743
57	A	5862.748	56	B	6654.574
58	A	5866.733	57	B	6713.430
59	A	5921.043	58	B	6736.093
60	A	5921.349	59	B	6775.099
61	A	5994.916	60	B	6797.267
62	A	6004.220	61	B	6800.953
63	A	6058.511	62	B	6808.889
64	A	6097.183	63	B	6920.187
65	A	6149.900	64	B	6926.273
66	A	6209.899	65	B	6969.694
67	A	6269.733	66	B	6998.157
68	A	6272.897	67	B	7067.384
69	A	6307.480			
70	A	6323.657			
71	A	6386.479			
72	A	6403.313			
73	A	6427.804			
74	A	6458.937			
75	A	6485.360			
76	A	6546.603			
77	A	6565.017			
78	A	6573.722			
79	A	6619.635			
80	A	6645.405			
81	A	6705.681			
82	A	6748.764			
83	A	6775.526			
84	A	6782.726			
85	A	6864.239			
86	A	6886.688			
87	A	6900.801			
88	A	6946.007			
89	A	6969.279			
90	A	6992.778			
91	A	7018.842			

Appendix E. Vibrational band centres for asymmetric ozone Cs isotopologues 16O18O18O and 16O16O18O using EKE Hamiltonian, DVR method and emprically optimised PES Tyuterev, Kochanov,Tashkun (model_mep1, September 2011)
All values in cm-1; Cut-off: 7000 cm-1

species	688		668
zpe	1384.157		1421.216
2 A'	677.652	2 A'	684.767
3 A'	993.744	3 A'	1027.918
4 A'	1060.667	4 A'	1090.279
5 A'	1352.746	5 A'	1366.893
6 A'	1656.708	6 A'	1696.849
7 A'	1730.866	7 A'	1767.276
8 A'	1962.561	8 A'	2028.584
9 A'	2025.257	9 A'	2046.366
10 A'	2027.620	10 A'	2090.321
11 A'	2113.213	11 A'	2172.402
12 A'	2316.706	12 A'	2362.653
13 A'	2398.401	13 A'	2441.520
14 A'	2611.103	14 A'	2682.022
15 A'	2680.778	15 A'	2723.131
16 A'	2695.173	16 A'	2748.848
17 A'	2776.095	17 A'	2841.764
18 A'	2903.230	18 A'	2998.834
19 A'	2967.961	19 A'	3025.263
20 A'	2973.678	20 A'	3060.599
21 A'	3055.683	21 A'	3112.875
22 A'	3063.154	22 A'	3148.072
23 A'	3157.911	23 A'	3246.172
24 A'	3256.275	24 A'	3331.835
25 A'	3330.511	25 A'	3397.131
26 A'	3362.436	26 A'	3403.758
27 A'	3436.007	27 A'	3508.056
28 A'	3537.527	28 A'	3636.954
29 A'	3603.927	29 A'	3684.529
30 A'	3627.504	30 A'	3700.547
31 A'	3699.439	31 A'	3781.142
32 A'	3724.952	32 A'	3796.656
33 A'	3809.317	33 A'	3907.610
34 A'	3814.011	34 A'	3932.954
35 A'	3883.132	35 A'	3977.977
36 A'	3898.043	36 A'	4002.496
37 A'	3969.440	37 A'	4054.522
38 A'	3976.433	38 A'	4068.400
39 A'	4027.007	39 A'	4092.424
40 A'	4077.767	40 A'	4170.875
41 A'	4092.558	41 A'	4198.804
42 A'	4168.056	42 A'	4270.923
43 A'	4194.294	43 A'	4311.152
44 A'	4235.956	44 A'	4335.947
45 A'	4278.068	45 A'	4340.574
46 A'	4338.406	46 A'	4440.201
47 A'	4383.527	47 A'	4446.021
48 A'	4429.220	48 A'	4553.856
49 A'	4465.461	49 A'	4566.628
50 A'	4502.295	50 A'	4620.213
51 A'	4536.366	51 A'	4624.449
52 A'	4593.914	52 A'	4700.651

species	688		668	
53	A'	4618.008	53 A'	4720.235
54	A'	4678.214	54 A'	4736.730
55	A'	4688.822	55 A'	4824.215
56	A'	4711.921	56 A'	4829.396
57	A'	4744.893	57 A'	4838.966
58	A'	4766.099	58 A'	4900.794
59	A'	4794.988	59 A'	4908.507
60	A'	4841.980	60 A'	4964.364
61	A'	4863.606	61 A'	4967.541
62	A'	4864.127	62 A'	4992.537
63	A'	4925.188	63 A'	5016.136
64	A'	4964.434	64 A'	5077.204
65	A'	4971.081	65 A'	5106.999
66	A'	5038.428	66 A'	5114.113
67	A'	5044.530	67 A'	5171.331
68	A'	5092.516	68 A'	5219.310
69	A'	5111.359	69 A'	5241.120
70	A'	5118.984	70 A'	5242.654
71	A'	5171.277	71 A'	5259.277
72	A'	5211.746	72 A'	5340.889
73	A'	5222.298	73 A'	5341.382
74	A'	5254.459	74 A'	5367.246
75	A'	5281.351	75 A'	5402.086
76	A'	5337.881	76 A'	5428.359
77	A'	5347.798	77 A'	5468.801
78	A'	5370.010	78 A'	5481.529
79	A'	5390.466	79 A'	5512.865
80	A'	5419.415	80 A'	5527.223
81	A'	5466.425	81 A'	5593.569
82	A'	5484.856	82 A'	5613.615
83	A'	5488.214	83 A'	5622.317
84	A'	5511.012	84 A'	5640.628
85	A'	5568.608	85 A'	5679.434
86	A'	5574.668	86 A'	5704.923
87	A'	5594.708	87 A'	5728.075
88	A'	5609.248	88 A'	5763.165
89	A'	5656.222	89 A'	5771.571
90	A'	5688.837	90 A'	5783.682
91	A'	5714.229	91 A'	5850.702
92	A'	5726.865	92 A'	5868.018
93	A'	5742.402	93 A'	5869.537
94	A'	5754.980	94 A'	5894.501
95	A'	5802.965	95 A'	5921.162
96	A'	5821.702	96 A'	5953.569
97	A'	5826.583	97 A'	5974.819
98	A'	5861.879	98 A'	6001.877
99	A'	5880.527	99 A'	6012.662
100	A'	5884.695	100 A'	6026.132
101	A'	5947.823	101 A'	6064.322
102	A'	5954.832	102 A'	6084.496
103	A'	5976.955	103 A'	6118.089
104	A'	6003.822	104 A'	6120.908
105	A'	6021.175	105 A'	6132.432
106	A'	6045.975	106 A'	6152.675
107	A'	6054.917	107 A'	6213.564
108	A'	6099.176	108 A'	6217.120
109	A'	6103.249	109 A'	6254.389
110	A'	6109.367	110 A'	6269.186
111	A'	6120.900	111 A'	6276.706

species	688		668
112 A'	6168.759	112 A'	6284.233
113 A'	6204.747	113 A'	6318.919
114 A'	6208.286	114 A'	6325.377
115 A'	6208.424	115 A'	6367.719
116 A'	6241.832	116 A'	6390.955
117 A'	6264.461	117 A'	6412.756
118 A'	6281.433	118 A'	6414.426
119 A'	6326.379	119 A'	6458.080
120 A'	6333.083	120 A'	6466.992
121 A'	6333.227	121 A'	6486.187
122 A'	6344.380	122 A'	6502.593
123 A'	6379.866	123 A'	6525.780
124 A'	6387.046	124 A'	6526.696
125 A'	6426.189	125 A'	6558.110
126 A'	6431.949	126 A'	6566.537
127 A'	6436.690	127 A'	6599.585
128 A'	6476.491	128 A'	6613.519
129 A'	6493.409	129 A'	6619.542
130 A'	6506.971	130 A'	6650.911
131 A'	6540.152	131 A'	6679.465
132 A'	6552.877	132 A'	6723.221
133 A'	6585.065	133 A'	6727.193
134 A'	6594.326	134 A'	6732.234
135 A'	6628.424	135 A'	6738.088
136 A'	6633.373	136 A'	6778.168
137 A'	6656.733	137 A'	6784.872
138 A'	6665.733	138 A'	6797.759
139 A'	6671.100	139 A'	6840.643
140 A'	6691.030	140 A'	6846.628
141 A'	6708.882	141 A'	6863.919
142 A'	6731.661	142 A'	6882.308
143 A'	6731.966	143 A'	6891.455
144 A'	6759.847	144 A'	6910.579
145 A'	6796.557	145 A'	6914.927
146 A'	6798.973	146 A'	6923.511
147 A'	6815.875	147 A'	6972.412
148 A'	6831.023	148 A'	6989.318
149 A'	6842.846	149 A'	7000.020
150 A'	6865.500	150 A'	
151 A'	6872.041	151 A'	
152 A'	6912.322	152 A'	
153 A'	6922.913	153 A'	
154 A'	6933.713	154 A'	
155 A'	6937.201	155 A'	
156 A'	6961.431	156 A'	
157 A'	6968.432	157 A'	
158 A'	6974.431	158 A'	
159 A'	7025.467	159 A'	